

Strongly confined excitons in self-assembled InGaAs quantum dot clusters produced by a hybrid growth method

Megan Creasey,¹ Xiaoqin Li,^{1,a)} J. H. Lee,² Zh. M. Wang,³ and G. J. Salamo³

¹Department of Physics, University of Texas, Austin, Texas 78712, USA

²Department of Electrical Engineering, Kwangwoon University, Seoul 139-701, South Korea

³Institute of Nanoscale Science and Engineering, University of Arkansas, Fayetteville, Arkansas 72701, USA

(Received 16 September 2009; accepted 20 February 2010; published online 18 May 2010)

We investigate the optical properties of newly developed InGaAs quantum dot clusters (QDCs). The QDCs are produced using a hybrid growth method that combines droplet homoepitaxy and Stranski–Krastanov growth modes. We focus on a particular geometry, where six individual quantum dots (QDs) spontaneously form a structure morphologically similar to a benzene ring. We observe narrow exciton resonances in microphotoluminescence measurements. Temperature and excitation density dependence of the exciton resonances are investigated. Our experiments suggest that excitons are strongly confined in individual QDs instead of residing in all QDs in the cluster.

© 2010 American Institute of Physics. [doi:10.1063/1.3369389]

Self-assembled quantum dots (QDs) grown by molecular beam epitaxy (MBE) exhibit interesting physical properties due to quantum confinement of excitons. For example, these QDs show isolated exciton resonances that resemble optical spectra from atoms.^{1,2} Additionally, Rabi oscillations between the ground state and exciton states have been observed when the exciton population is coherently driven by ultrafast optical pulses.³ When exciton resonances are coupled to optical cavity modes, phenomena such as the Purcell effect and Rabi vacuum splitting have been demonstrated.^{4–6} QDs are considered a promising candidate for a wide range of applications based on these properties—from conventional optoelectronic devices, such as photon-detectors and lasers, to novel applications, such as single photon sources^{7,8} and quantum logic gates.⁹

For many applications, it is desirable to fabricate organized QD arrays with chosen spatial frequencies. However, an “exclusive growth zone” seems to exist in some cases, i.e., QDs cannot be grown at arbitrarily close distances to each other. To continue the miniaturization of electronic and optoelectronic devices it is necessary to circumvent this limitation. One approach is to explore QD clusters (QDCs). A QDC is a group of QDs arranged in a chosen geometry. In addition to increased device density, QDCs potentially allow controllable couplings between individual QDs. Such controlled coupling could lead to interesting new applications. For example, a two-bit quantum gate requires two interacting logic-qubits, and each logic-qubit requires five or more physical qubits for error corrected operations.^{10,11}

Self-assembled QDs produced using the Stranski–Krastanov (SK) growth method^{1,12} have been extensively studied. As grown, these samples typically consist of isolated QDs with random spatial placements. Various methods have been developed to synthesize QDCs based on the SK growth mode, including strain engineering,^{13,14} strain enhanced etching,¹⁵ and lithographic patterning.^{16–20} These methods,

however, either involve *ex situ* surface preparation or require additional processing steps that add to the complexity of fabrication processes. The QDCs we investigate in this paper are produced by a hybrid growth method combining droplet homoepitaxy and SK growth modes. A variety of QDC geometries can be produced using this method. The most complex QDC produced by this growth method so far is a benzene ring type of structure, in which each QDC comprises six individual QDs, as shown in Fig. 1. We focus on the optical properties of this particular type of QDC in this report.

We first describe the growth procedure briefly.^{21–23} The QDCs were grown on epi-ready semi-insulated GaAs (100) substrates using MBE. To grow a defect-free GaAs buffer, native gallium oxide was desorbed by annealing substrates at 610 °C for 10 min. After annealing, 500 nm of homoepitaxial GaAs buffer was grown at 610 °C at a growth rate of 0.75 monolayers per second (ML/s). Subsequently, the substrate was annealed *in situ* for 3 min to equilibrate the surface matrix. The substrate temperature (T_{sub}) was then quenched to 150 °C for creation of liquid Ga droplets using

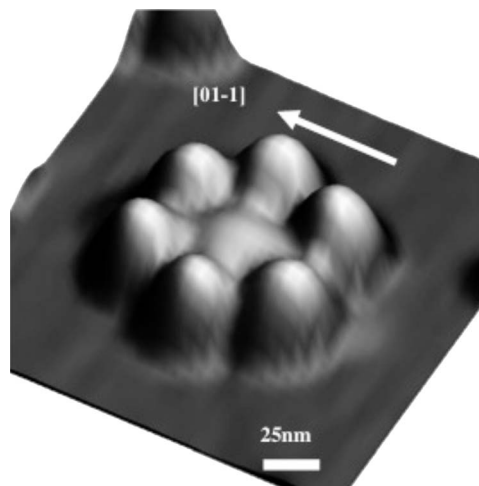


FIG. 1. An AFM image (250 nm × 250 nm) of a typical hexa-QDC.

^{a)}Electronic mail: elaineli@physics.utexas.edu.

the Volmer–Weber growth mode.²⁴ Immediately after the formation of droplets, a beam equivalent pressure (BEP) of 1.3×10^{-5} Torr of As₄ was used to convert them into GaAs nanoislands. For fabrication of the QDCs, the T_{sub} was increased to 500 °C and 2.0 MLs of InAs were deposited under a BEP of 3.4×10^{-6} Torr of As₄. For morphological measurements, the T_{sub} was quenched right after the formation of QDCs. For optical measurements, a 200 ML GaAs capping layer was added. A typical atomic force microscopy (AFM) image of the sample is shown in Fig. 1. The figure shows a 250 nm × 250 nm three-dimensional image of a QDC. Each QDC resides on a flat InGaAs base with a height of ~ 4 nm. The QDC was slightly elongated along $[01\bar{1}]$ with an aspect ratio of ~ 1.3 . This particular cluster is approximately 230 nm along $[01\bar{1}]$ and 175 nm along $[011]$ measured as the semimajor and semiminor axes of the ellipse enclosing the QDs. The height of individual QDs ranges from 9 to 12 nm and varies among dots within the same cluster. The average interdot distance was 50–70 nm.

Although there have been several reports on the growth mechanisms and structural characterization of these newly developed QDCs, no previous studies have characterized their optical properties. In this paper, we report photoluminescence (PL) measurements at both ensemble and single cluster levels. For these measurements, the sample was mounted on the cold finger of a liquid helium cryostat, and the temperature was held at ~ 8 K unless noted specifically. A 532 nm, continuous-wave laser incident from an oblique angle was focused onto the sample with a lens (focal length = 10 cm). The spot size of the excitation beam at the sample surface was tens of microns in diameter. For ensemble measurements, we used a collection lens with a 6 cm focal length. For measurements on the single cluster level, we used a 100×, long working distance microscope objective with 0.5 NA. The collected PL was then sent to a 0.55 m long imaging spectrometer, which enables one to further distinguish individual exciton emission lines via spatial and spectral dispersion. The spectra were recorded using a liquid nitrogen-cooled, back-illuminated Si charged coupled detector (CCD).

An AFM image of the uncapped sample [Fig. 2(a)] shows a high QDC density (approximately 5×10^8 cm⁻²). We first captured a spatial image using the CCD camera by setting the spectrometer entrance at 2 mm and the grating at the zeroth order. As shown in Fig. 2(b), individual clusters cannot be spatially resolved in the optical image. To isolate individual exciton resonances, one can perform measurements exploiting both spectral and spatial dispersion. A spectrum was taken at a lower excitation power of 0.1 mW, with a 150 g/mm grating and 16 μ m slit-width, as shown in Fig. 2(c). PL signals along the same horizontal row on the CCD image come from the same vertical position on the sample. We display the signal along a single row (indicated by the arrows) of the CCD image in Fig. 2(d) as the solid line. The line shape matches a separate ensemble measurement (the dotted line) very well with the peak intensities normalized. Three isolated, narrow transitions are observed in the higher energy region and displayed in the inset as measured with a

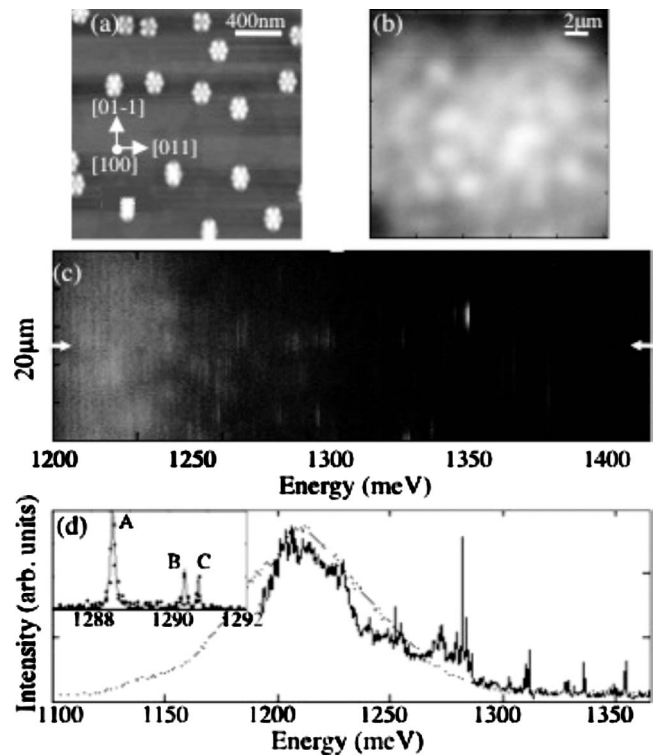


FIG. 2. (a) An AFM image of the sample prior to addition of the GaAs capping layer. (b) Spatial image of sample taken using micro-PL setup. (c) Micro-PL data taken from the area shown in (b). (d) Dotted line shows an ensemble measurement. Solid line shows PL intensity from a single row indicated by arrows in (c). Inset: Lorentzian line fit to isolated resonances at higher energy end of the spectrum.

1200 g/mm grating. The solid lines are Lorentzian functions fit to the data. The extracted full width at half maximum linewidth (FWHM) is 0.127 meV for peak A, 0.073 meV for Peak B, and 0.071 meV for peak C. The resonances B and C exhibit a linewidth close to the instrument resolution of 0.05 meV.

In principle, the PL linewidth from single emitters is determined by the homogeneous linewidth, which is inversely proportional to the dephasing time T_2 . Due to the long integration time (5 min) of micro-PL measurements, the measured linewidth could be broadened by various mechanisms, such as charge fluctuation.²⁵ The apparent linewidth, therefore, only provides an upper bound for the intrinsic homogeneous linewidth. A linewidth of ~ 0.07 meV corresponds to a dephasing time (T_2) of ~ 10 ps. The dephasing time is related to the lifetime (T_1) by $1/T_2 = 1/(2T_1) + \gamma_{\text{pure}}$, where γ_{pure} represents the rate of pure dephasing processes, and the lifetime is determined by a combination of radiative and nonradiative decay processes.

Since the InGaAs QDs in this study evolve from a single GaAs nanoisland during the growth process, a legitimate question is whether optically excited excitons are confined in individual QDs. We found the lifetime, T_1 , to be around 400 ps in time-resolved PL measurements (data not included). This lifetime is comparable to that measured in typical isolated InAs/GaAs QDs grown in the SK mode.²⁶ This comparable exciton lifetime suggests that the excitons in our sample are localized in individual QDs, not in the entire cluster. If the excitons were weakly confined in the whole

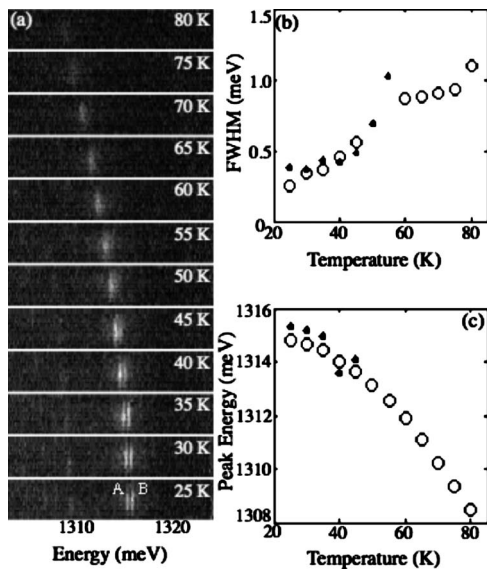


FIG. 3. (a) Evolution of PL with increasing temperature. (b) Linewidth of resonances shown in (a). (c) Center wavelength of resonances shown in (a). (b) and (c) are values obtained from Lorentzian fits to integrated intensity data. In plots (b) and (c), empty circles represent peak A and filled circles represent peak B.

cluster, one would expect the dipole moment, the radiative decay rate, and, therefore, the lifetime to be drastically different.

Next, we investigated the dependence of single exciton resonances on temperature (Fig. 3). A series of spectra were taken in the temperature range from 25 to 80 K. Both a pronounced redshift in the peak position and a broadening in the linewidth were observed as the temperature was increased [Fig. 3(a)]. Although the intensity of the emissions decreased with increasing temperature, isolated resonances were still detectable at 80 K with integration times of a few minutes. For exciton resonances to be observed, the exciton binding energy should be larger than the thermal energy. At 80 K, thermal energy is about 7 meV. The exciton binding energy decreases quickly as the lateral dimension of the QDs increases. The electronic levels and exciton binding energies for typical InAs/GaAs QDs grown using the SK mode have previously been calculated.²⁷ For a QD with 6 nm height, the exciton binding energy drops from ~ 27 meV for lateral sizes of 6 nm to ~ 12 meV for lateral sizes of 19 nm. If the excitons were confined in the whole cluster in our sample, the exciton binding energy would approach the theoretical limit in two dimensional InAs (~ 4 meV).²⁸ The observation of exciton resonances in our sample at high temperature further supports the conclusion that the excitons are strongly confined in individual QDs in the cluster. The change in linewidth as a function of temperature is examined in detail in Fig. 3(b). The linewidth increases from 0.25 meV at 25 K to 1.09 meV at 80 K for peak A. This increase in linewidth is due to increased electron-phonon interaction at higher temperatures. The spectral shift as a function of temperature follows a quadratic function, as shown in Fig. 3(c). This trend is consistent with previous studies performed on self-assembled InGaAs QDs grown in the SK mode.²⁹ This spec-

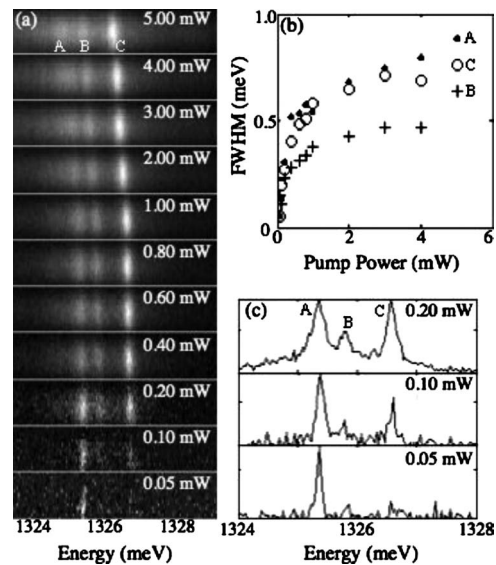


FIG. 4. (a) Evolution of exciton resonances with increasing pump power. (b) Linewidth dependence on pump power for three resonances shown in (a) as measured by a Lorentzian fit to the integrated spectrums. (c) Integrated intensity of three lowest energy spectrums shown in (a).

tral shift is typically attributed to the band gap changes in bulk InAs and GaAs.

Lastly, we studied the dependence of exciton resonances on excitation power, as shown in Fig. 4. In addition to a small spectral shift, the linewidth broadens from 0.11 meV at a pump power of 50 μ W to as large as 1.6 meV at 5 mW, as shown in Fig. 4(b). The local temperature under the laser excitation spot, however, likely rose as the excitation power was increased. The changes in spectral position and linewidth are consistent with a temperature rise at higher excitation powers. We examine the intensity change for exciton resonances in the low excitation power regime in more detail in Fig. 4(c). From these measurements, it is clear that resonance C increases faster than resonances A and B in this power regime. This power dependence suggests that this higher energy resonance may arise from biexcitons, though it is difficult to reliably associate a biexciton transition with the related exciton resonance based on PL measurements alone. If we assume that peak C is the biexciton associated with the exciton peak A, an antibinding energy of 1.2 meV can be extracted. In bulk materials, biexcitons typically occur at a lower energy than excitons since such biexcitons are energetically favorable. Biexcitons at a higher energy than the associated excitons have been previously reported in self-assembled QDs.³⁰ In this case, biexcitons form in the strong confining potential of the QD despite the fact that they occupy a higher energetic state.

In conclusion, we observed narrow PL lines from individual excitons localized in hexa-QDC produced by a new hybrid growth approach. Our measurements prove that these newly developed QDCs exhibit high optical quality. Narrow exciton resonances can be observed at temperatures as high as 80 K. Both the narrow exciton linewidth and the observation of exciton resonances at higher temperatures suggest that excitons are strongly confined in individual QDs, instead of being delocalized in all QDs in a cluster. Only strongly

confined excitons can be addressed individually to fulfill potential advantages offered by QDCs. In the near future, we intend to investigate possible couplings among individual QDs within the same QDC. Coupling between QDs has only been demonstrated in very limited geometries so far, i.e., between a pair of vertically aligned or planar QDs.^{31–33} QDCs with complex configurations such as those investigated in this report offer a promising planar geometry for scalable devices. Considering the relatively large spatial separation between individual QDs (tens of nanometers), an external electrical field is likely necessary to induce couplings between the QDs.

ACKNOWLEDGMENTS

The authors gratefully acknowledge the following agencies for funding: NSF (Grant No. DMR-0747822), ARO (Grant Nos. W911NF-08-1-0348 and W911NF-07-100223), ONR (Grant No. N00014-08-1-0745), AFOSR (Grant No. FA9550-10-1-002), the Welch Foundation (Grant No. F-1662), and the Alfred Sloan foundation. The work at Arkansas is supported by NSF under Grant No. DMR-0520550.

- ¹J. Y. Marzin, J. M. Gérard, A. Izraël, D. Barrier, and G. Bastard, *Phys. Rev. Lett.* **73**, 716 (1994).
- ²M. Bayer, O. Stern, P. Hawrylak, S. Fafard, and A. Forchel, *Nature (London)* **405**, 923 (2000).
- ³A. Zrenner, E. Beham, S. Stuffer, F. Findeis, M. Bichler, and G. Abstreiter, *Nature (London)* **418**, 612 (2002).
- ⁴E. Moreau, I. Robert, J. M. Gerard, I. Abram, L. Manin, and V. Thierry-Mieg, *Appl. Phys. Lett.* **79**, 2865 (2001).
- ⁵T. Yoshie, A. Scherer, J. Hendrickson, G. Khitrova, H. M. Gibbs, G. Rupper, C. Ell, O. B. Shchekin, and D. G. Deppe, *Nature (London)* **432**, 200 (2004).
- ⁶M. Bayer, T. L. Reinecke, F. Weidner, A. Larionov, A. McDonald, and A. Forchel, *Phys. Rev. Lett.* **86**, 3168 (2001).
- ⁷P. Michler, A. Imamoglu, M. D. Mason, P. J. Carson, G. F. Strouse, and S. K. Buratto, *Nature (London)* **406**, 968 (2000).
- ⁸Z. Yuan, B. E. Kardynal, R. M. Stevenson, A. J. Shields, C. J. Lobo, K. Cooper, N. S. Beattie, D. A. Ritchie, and M. Pepper, *Science* **295**, 102 (2002).
- ⁹X. Q. Li, Y. W. Wu, D. Steel, D. Gammon, T. H. Stievater, D. S. Katzer, D. Park, C. Piermarocchi, and L. J. Sham, *Science* **301**, 809 (2003).

- ¹⁰C. H. Bennett, D. P. DiVincenzo, J. A. Smolin, and W. K. Wootters, *Phys. Rev. A* **54**, 3824 (1996).
- ¹¹R. Laflamme, C. Miquel, J. P. Paz, and W. H. Zurek, *Phys. Rev. Lett.* **77**, 198 (1996).
- ¹²D. Leonard, M. Krishnamurthy, C. M. Reaves, S. P. Denbaars, and P. M. Petroff, *Appl. Phys. Lett.* **63**, 3203 (1993).
- ¹³H. Lee, J. A. Johnson, M. Y. He, J. S. Speck, and P. M. Petroff, *Appl. Phys. Lett.* **78**, 105 (2001).
- ¹⁴T. van Lippen, R. Nötzel, G. J. Hamhuis, and J. H. Wolter, *J. Appl. Phys.* **97**, 044301 (2005).
- ¹⁵S. Rudeesun, K. Suwit, and G. S. Oliver, *Appl. Phys. Lett.* **82**, 2892 (2003).
- ¹⁶M. H. Baier, C. Constantin, E. Pelucchi, and E. Kapon, *Appl. Phys. Lett.* **84**, 1967 (2004).
- ¹⁷M. H. Baier, S. Watanabe, E. Pelucchi, and E. Kapon, *Appl. Phys. Lett.* **84**, 1943 (2004).
- ¹⁸V. C. Elarde, R. Rangarajan, J. J. Borchardt, and J. J. Coleman, *IEEE Photonics Technol. Lett.* **17**, 935 (2005).
- ¹⁹S. Birudavolu, N. Nuntawong, G. Balakrishnan, Y. C. Xin, S. Huang, S. C. Lee, S. R. J. Brueck, C. P. Hains, and D. L. Huffaker, *Appl. Phys. Lett.* **85**, 2337 (2004).
- ²⁰P. S. Wong, G. Balakrishnan, N. Nuntawong, J. Tatebayashi, and D. L. Huffaker, *Appl. Phys. Lett.* **90**, 183103 (2007).
- ²¹J. H. Lee, Z. M. Wang, N. W. Strom, Y. I. Mazur, and G. J. Salamo, *Appl. Phys. Lett.* **89**, 202101 (2006).
- ²²K. A. Sablon, J. H. Lee, Z. M. Wang, J. H. Shultz, and G. J. Salamo, *Appl. Phys. Lett.* **92**, 203106 (2008).
- ²³J. H. Lee, K. Sablon, Z. M. Wang, and G. J. Salamo, *J. Appl. Phys.* **103**, 054301 (2008).
- ²⁴M. Volmer and A. Weber, *Z. Phys. Chem.* **119**, 277 (1926).
- ²⁵M. Bayer and A. Forchel, *Phys. Rev. B* **65**, 041308 (2002).
- ²⁶Y. Haiping, L. Sam, R. Christine, and M. Ray, *Appl. Phys. Lett.* **69**, 4087 (1996).
- ²⁷M. Grundmann, O. Stier, and D. Bimberg, *Phys. Rev. B* **52**, 11969 (1995).
- ²⁸H. Mathieu, P. Lefebvre, and P. Christol, *Phys. Rev. B* **46**, 4092 (1992).
- ²⁹A. Kiraz, P. Michler, C. Becher, B. Gayral, A. Imamoglu, L. Zhang, E. Hu, W. V. Schoenfeld, and P. M. Petroff, *Appl. Phys. Lett.* **78**, 3932 (2001).
- ³⁰R. J. Young, R. M. Stevenson, A. J. Shields, P. Atkinson, K. Cooper, D. A. Ritchie, K. M. Groom, A. I. Tartakovskii, and M. S. Skolnick, *Phys. Rev. B* **72**, 113305 (2005).
- ³¹G. Schedelbeck, W. Wegscheider, M. Bichler, and G. Abstreiter, *Science* **278**, 1792 (1997).
- ³²M. Bayer, P. Hawrylak, K. Hinzer, S. Fafard, M. Korkusinski, Z. R. Wasilewski, O. Stern, and A. Forchel, *Science* **291**, 451 (2001).
- ³³G. J. Beirne, C. Hermannstadter, L. Wang, A. Rastelli, O. G. Schmidt, and P. Michler, *Phys. Rev. Lett.* **96**, 137401 (2006).